NASA TECHNICAL NOTE

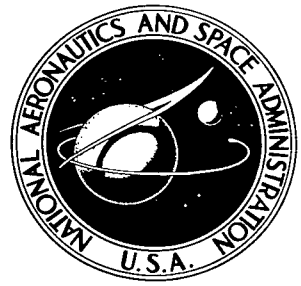

NASA TN D-8494 c.1

NASA TN D-8494

MESOSCALE CLOUD PHENOMENA OBSERVED BY LANDSAT

James P. Ormsby

Goddard Space Flight Center

Greenbelt, Md. 20771

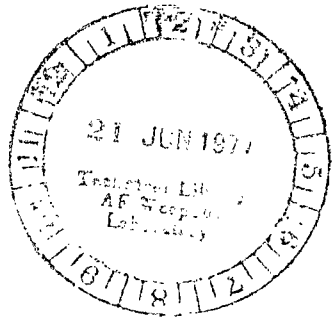

NATIONAL AERONAUTICS AND SPACE ADMINISTRATION • WASHINGTON, D. C. • JUNE 1977

1. Report No.	2. Government Accession No.	3. Recipient's Catalog No.
TND-8494		

4. Title and Subtitle

Mesoscale Cloud Phenomena Observed by Landsat

5. Report Date: June 1977

6. Performing Organization Code: 913

7. Author(s): James P. Ormsby

8. Performing Organization Report No.: G-7702 F14

9. Performing Organization Name and Address

Goddard Space Flight Center
Greenbelt, Maryland 20771

10. Work Unit No.: 177-54-41

11. Contract or Grant No.

13. Type of Report and Period Covered: Technical Note

12. Sponsoring Agency Name and Address

National Aeronautics and Space Administration
Washington, D.C. 20546

14. Sponsoring Agency Code

15. Supplementary Notes

16. Abstract

Examples of certain mesoscale cloud features, for example, jet cirrus, eddies/vortices, cloud banding, and wave clouds have been collected from Landsat imagery and placed into Mason's four groups of causes of cloud formation based on the mechanism of vertical motion which produces condensation. These groups are as follows: 1) layer clouds formed by widespread regular ascent; 2) layer clouds caused by irregular stirring motions; 3) convective clouds; and 4) clouds formed by orographic disturbances. These mechanisms explain general cloud formation. Once formed, other forces may play a role in the deformation of a cloud or cloud mass into unusual and unique meso- and microscale patterns. Each example presented is followed by a brief discussion in this report describing the synoptic situation, and some inference into the formation and occurrence of the more salient features. No major attempt has been made to discuss in detail the meteorological and topographic interplay producing these mesoscale features.

17. Key Words (Selected by Author(s))	18. Distribution Statement
Landsat, Mesoscale and Microscale cloud patterns	Unclassified–Unlimited Cat. 47

19. Security Classif. (of this report)	20. Security Classif. (of this page)	21. No. of Pages	22. Price*
Unclassified	Unclassified	32	$4.00

*For sale by the National Technical Information Service, Springfield, Virginia 22161.

This document makes use of international metric units according to the Systeme International d'Unites (SI). In certain cases, utility requires the retentions of other systems of units in addition to the SI units. The conventional units stated in parentheses following the computed SI equivalents are the basis of the measurements and calculations reported.

CONTENTS

MESOSCALE CLOUD PHENOMENA OBSERVED BY LANDSAT

James P. Ormsby
Goddard Space Flight Center
Greenbelt, Maryland

INTRODUCTION

Landsat-1 was originally launched for "the acquisition of synoptic, multispectral repetitive images . . . from which useful data can be obtained for investigations in such disciplines as: agriculture, geology, geography, hydrology, ecology, and oceanography" (Reference 1). Numerous frames contain greater than 30-percent cloud cover, which is considered to be the nominal ground observation limit of usability for Earth resources applications. As a result, although many frames are unusable for the above purposes, many offer detailed (approximately 80-m resolution) views of meso- and microscale features, making them ideal for the study of lee waves, cloud streets, orographic and differential heating effects, and coastal stratus.

Landsat applicability is limited, however, because coverage is spatially restricted to a 185-km wide data swath, and temporally limited to coverage once every 18 days over a given area.*

The four-channel multispectral scanner subsystems (MSS) on both Landsat-1 and -2 utilize the 0.5- to 1.1-μm portion of the electromagnetic spectrum (0.5 to 0.6, 0.6 to 0.7, 0.7 to 0.8, 0.8 to 1.1 μm), with the region from 0.6 to 0.7 μm being best suited for sensing clouds because it is less susceptible to saturation caused by the high reflectivity of the clouds.

Clouds are generally classified by meteorologists by their appearance based on an international system (Reference 2) similar to that proposed by Luke Howard approximately 150 years ago (Reference 3). However, a cloud's appearance (dimensions and shape) is largely influenced by different kinds of air movements. This allows one to classify cloud features based on the dynamics which produce them.

Mason (Reference 3) indicates four such mechanisms:

- Layer clouds formed by widespread regular ascent
- Layer clouds caused by irregular stirring motions
- Convective clouds
- Clouds formed by orographic disturbances

*With the original launch of Landsat-2 there was coverage every 9 days for limited periods. Orbital adjustments to Landsat-1 made during 1977 provide alternate 6- and 12-day intervals between coverage.

The various Landsat scenes which follow have been arranged as much as possible into Mason's four groups. These scenes depict a few of the striking meso- and microscale cloud phenomena taken by Landsat-1 since its successful launch on July 23, 1972. While the above four mechanisms help explain cloud formation in general, once formed, a cloud or cloud mass may be deformed by other forces into unusual and unique meso- and microscale patterns. From the many available cloud features of interest, several have been selected for each mechanism, and their associated dynamics briefly discussed.

LAYER CLOUDS FORMED BY WIDESPREAD REGULAR ASCENT

This group of clouds is formed by slow, prolonged ascent throughout a deep layer of air, and is associated with cyclonic depressions near fronts and in other bad-weather systems. While most high cirrus clouds are primarily due to regular ascent, their pattern is often determined by nonlocalized wave disturbances, such as jet streams, which eventually trigger their formation. Therefore, an example of jet cirrus is included with such other features as island wake effects, shock waves, and eddies/vortices.

A jet stream produces certain characteristic cloud forms and types which make it easy to find its location on satellite imagery. The main jet-stream cloud features are long shadow lines, large cirrus shields with sharp boundaries, long cirrus bands, cirrus streaks, and transverse bands within cirrus cloud formations. These are the result of vertical and horizontal motions in the upper troposphere near the maximum wind zone (Reference 4).

Due to the small (185- by 185-km) synoptic view offered by Landsat, only a small portion of a jet-stream cloud formation can be seen. Figure 1 shows a portion of jet-stream clouds observed by Landsat-1 over the coasts of North and South Carolina. The winds were out of the southwest ranging from 77.2 to 92.6 m/s (150 to 180 knots). Athens, Georgia; Cape Hatteras, North Carolina; and Norfolk, Virginia reported 300-mb winds of 84.8, 77.2, and 92.6 m/s (165, 150, and 180 knots), respectively, with wind values decreasing northward and southward of a mean line through these points. This indicates that the main jet lies poleward of the shadows caused by the cirrus streaks. Anderson et al., (Reference 4) state that "the poleward boundary of the cirrus is often very abrupt; and lies under or slightly equatorward from the jet axis."

Numerous long cirrus bands comprise a portion of the feature shown in figure 1. Some of the thinner bands to the north consist of transverse lines. These lines are called cloud trails and are usually associated with wind speeds of 41.2 m/s (80 knots) or higher (Reference 4). Due to the thinness of the poleward bands, a distinct long poleward shadow is made up of numerous shadows (A to A). As a result of the increased resolution, one may be seeing some bands which would not be seen by lower resolution instruments. There is no extensive lower cloud deck upon which the jet cirrus can cast its shadow. The major part of the shadow is cast on the land or water surface with only a slight shadow visible on a lower cloud deck, C.

Three distinct cloud layers are visible: a lower stratocumulus layer, B, upon which is cast a thin shadow from a higher, possibly altocumulus deck, and then the shadow on the middle layer, C, cast by the thinner cirrus bands.

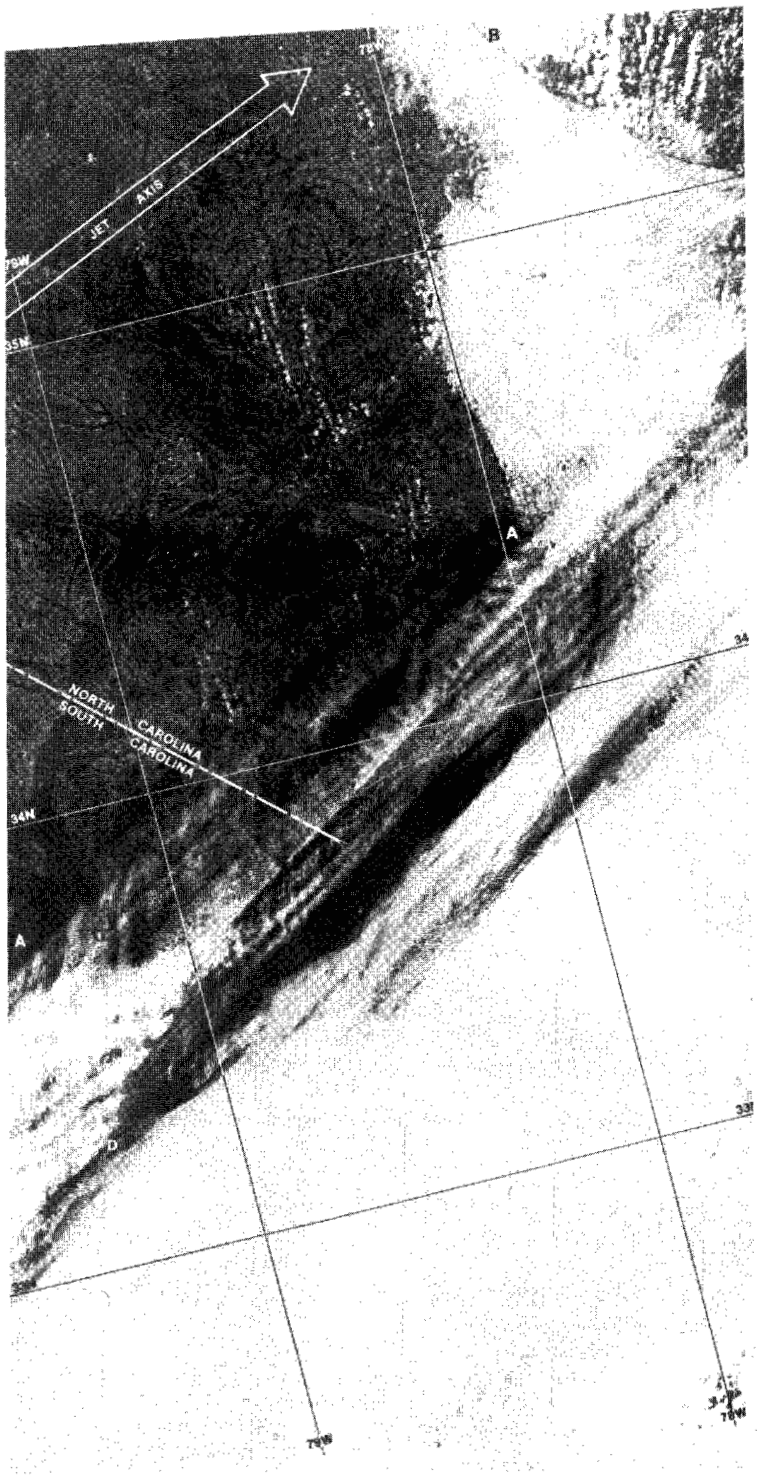

Figure 1. Jet cirrus off the North and South Carolina coasts (Landsat-1, February 9, 1974, 1566 - 15162, 15165).

In figure 2, a large high was situated to the west of the area, producing 5.1- to 7.7-m/s (10- to 15-knot) winds out of the northwest. On the eastern side of anticyclones, a low-level inversion tends to occur, resulting from subsidence aloft. The greater low-level stability would tend to favor stratus type clouds that can exhibit features which show the turbulence produced in the wake of the islands.

The eddies/vortices shown in figure 2 occurred in the northern midlatitudes in the Aleutian Islands chain, and are representative of the disruptive effect the islands of Amukta, Chagulak, and Yunaska of the Aleutian Islands chain have on the airflow around them. Over 85 km downwind of Amukta, eddies still persisted, with the larger eddies estimated to be up to 4 km in diameter. Chopra and Hubert (Reference 5) state that "a vortex street develops behind an obstacle when the flow in the wake region does not mix with that in the surrounding region. The transfer of momentum between the wake and basic flow region is minimized, thereby contributing to the long lifetime and persistence downstream."

The eddies/vortices to the lee of Amukta observed by Landsat-1 fit the Kármán vortex street pattern observed in laboratory investigations of wake behind an obstacle. The vortices arrange themselves in a double-row pattern in which each eddy/vortex is centered between the eddies/vortices in the other row.

The ratio of the lateral spacing (h) between the two vortex rows and the longitudinal spacing (a) of the eddies/vortices in the same row have been observed to have values in the range $0.28 < h/a < 0.52$, depending on the shape of the body, flow characteristics, and the distance downstream (Reference 5). In this particular instance, the approximate values for h and a were 4.5 and 10.5 km, respectively, given a ratio of 0.43, which falls between the values observed in the laboratory. Disturbances created by Chagulak and Yunaska are not as striking. This may possibly be due to the cloud depth in relation to the island elevation. The high point of Amukta is several hundred feet greater than that of Yunaska Island.

In figure 3, the Andreanof Islands, a portion of the Aleutian chain, disrupt an otherwise rather uniform cloud deck to form clear areas. These clear areas are a result of the mixing of the atmosphere downwind of the islands as the air flows around the higher land features. A high was situated south of the area producing a light 2.6- to 5.1-m/s (5- to 10-knots) breeze from the west. In the case of Gareloi Island, an unique scallop-shaped wake pattern has been set up which damps out about 123 km downwind as measured from the windward side of the island. East of Gareloi Island is Tanaga Island which has produced a conical-shaped wake, leaving most of the island cloud-free. The high points of these two islands are evidenced by snow-capped peaks. The southern portion of Kanaga Island has no high land masses, but the change in frictional effects between water and the high land surface has resulted in the formation of some waves in the stratus deck. Also, some vortex patterns appear southeast of Kanaga Island.

Figure 4 covers a portion of the Island of Newfoundland and most of the Avalon Peninsula. At 1200 Greenwich mean time (GMT), a large high (1036 mb) was situated northeast of the area with a cold front approaching from the west. Winds were out of the south southwest ranging from 5.1 to 10.3 m/s (10 to 20 knots) at the surface. With increased altitude, the

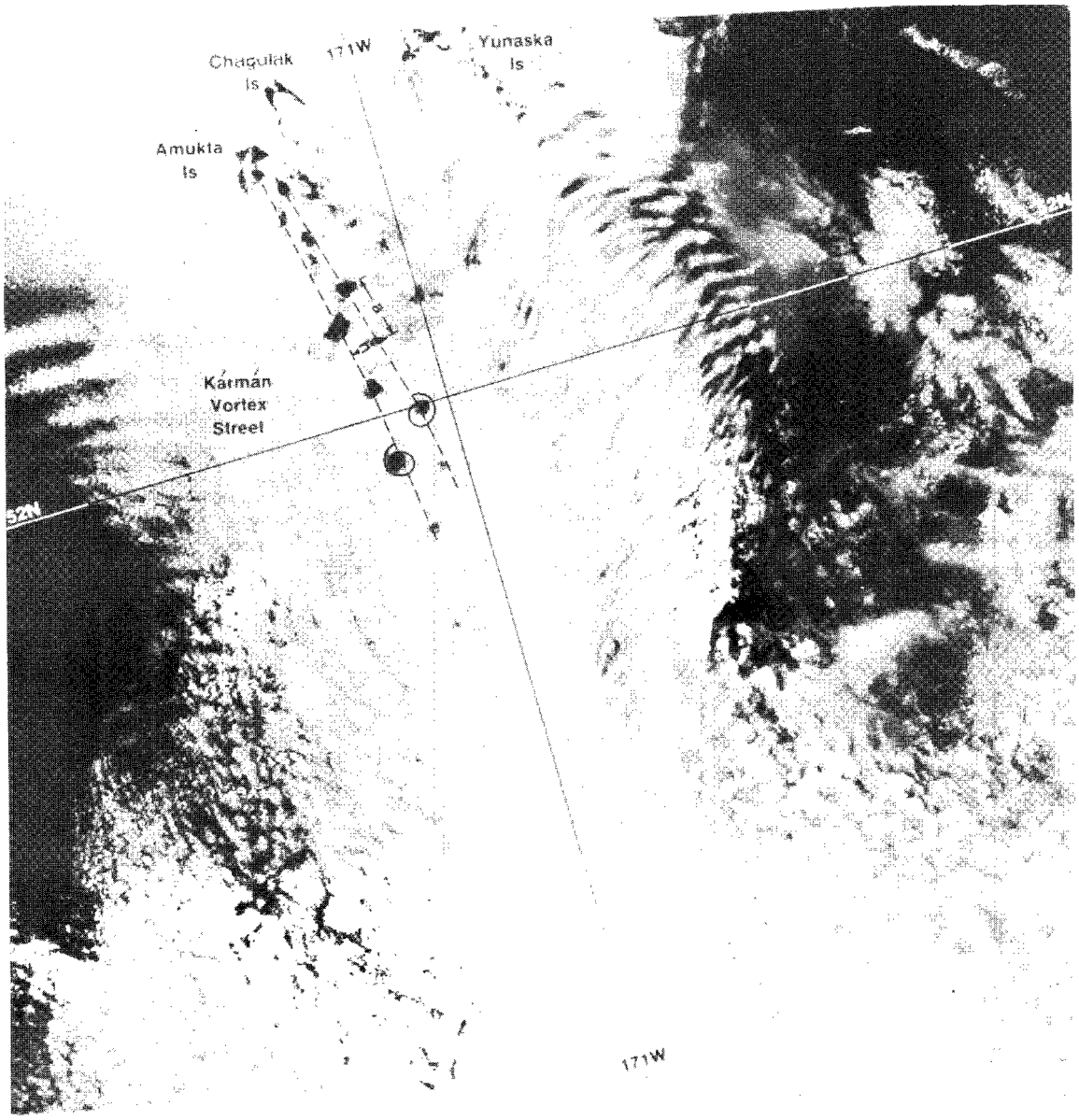

Figure 2. Kármán vortex street induced by Amukta Island (Landsat-1, June 17, 1973, 1329-21514).

Figure 3. Island wakes in stratus deck caused by islands in the Aleutian chain (Landsat-1, November 13, 1973, 1478-22180).

winds remained fairly constant with height. The winds were 15.4 m/s (30 knots) from the southwest through the 500-mb level.

Two distinct cloud types exist in figure 4: stratus clouds appear along the southeast coasts, 'A,' of the land masses, while over land, cumulus bands (streets) exist. The wind appears to have piled the stratus up along the coasts, with Cape St. Mary's and Cape Pine forming the focal point of large shock waves. Smaller shock waves can be seen where the land projects into the airflow, and atmospheric conditions are favorable for cloud formation.

The fact that this was a situation occurring during the midsummer helps explain the abrupt change in clouds formed over water and land. The land, which has a lower heat capacity, had heated up more quickly than the water, thereby increasing the potential for convective activity. In addition to the higher heat capacity of the water, the cold Labrador current flowing southward east of Avalon Peninsula would tend to stabilize the lower atmosphere, further increasing stratus development.

Within the stratus layers, small (microscale) waves can be seen. Reiter (Reference 6) places all features below 10^4 horizontal meters within the microscale. These waves, for the most part, have wavelengths ranging up to 1 km. These waves are oriented normal to the wind flow. While they are over the land areas, the cumulus cloud streets are oriented parallel to the airflow. These streets, at the point of origin, are approximately 1-km apart, increasing to 3-km, and in some cases 6- to 8-km apart before disappearing over water or coming to the end of the image.

Figure 5 shows another example of shock waves. These occurred on August 21, 1972, as a result of the disruption of the low-level flow by the Diomede Islands, located between the USSR and Alaska. Winds reported at 1800 GMT along the Alaskan coast ranged from 5.1 to 7.7 m/s (10 to 15 knots) from the northeast. The airflow over the two islands, though, was more from the north, based on the appearance of the shock-wave pattern. Leeward of the islands, standing waves were propagated, producing wave clouds which extended tens of kilometers downwind. The wavelength between the two waves immediately adjacent to Little Diomede was approximately 3 km, decreasing to 1.5 km downstream. Elsewhere, numerous wave formations can be seen.

Numerous small-scale spiral-like cloud formations appear in Landsat images. Figure 6 shows a portion of the eastern coast of Spain and southern France with a vortex along the coast. These patterns may exist at any cloud level ranging in size from the mesoscale eddies of 18.5 to 185.2 km (10 to 100 nmi) (see figure 2) which occur downwind from island barriers, to the subsynoptic scale (185.2 to 555.6 km (100 to 300 nmi)) spiral patterns occurring in stratocumulus clouds near coastlines (Reference 7). If this frame were of a larger scale, the pattern would look much like the occluded wave or occluding cyclone stage of the cyclone model proposed by Boucher and Newcomb (Reference 8). In their case, the clear area between the tightly wound spiral and the outer arm was caused by cooler, drier air entering the system. In this case, as Anderson et al., (Reference 7) indicate, subsynoptic and mesoscale vortices should not be confused with the larger scale phenomena, since they generally result from different mechanisms and do not represent a potential for development.

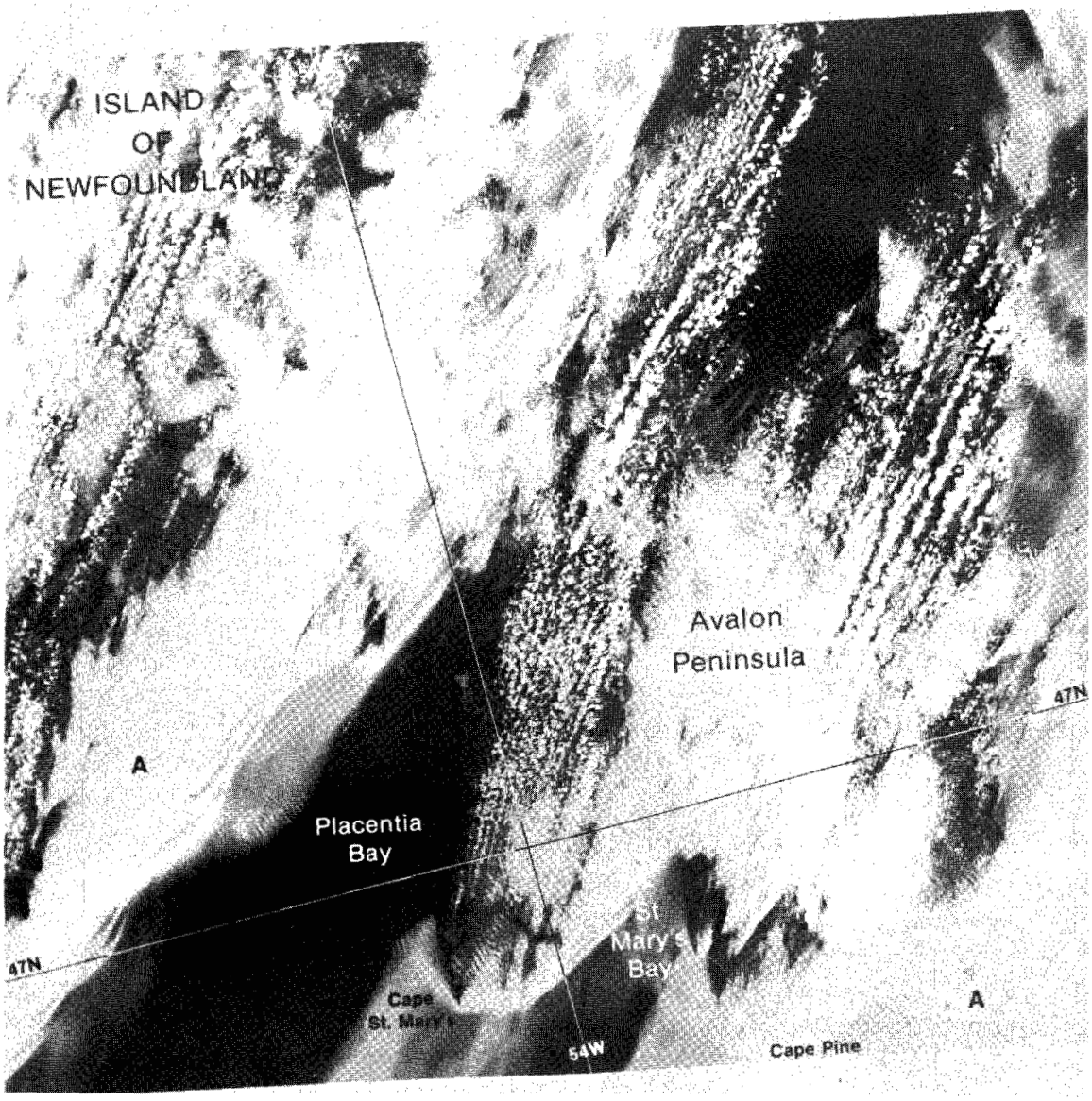

Figure 4. Shock waves off the South Avalon Peninsula (Landsat-1, July 30, 1973, 1372-13562).

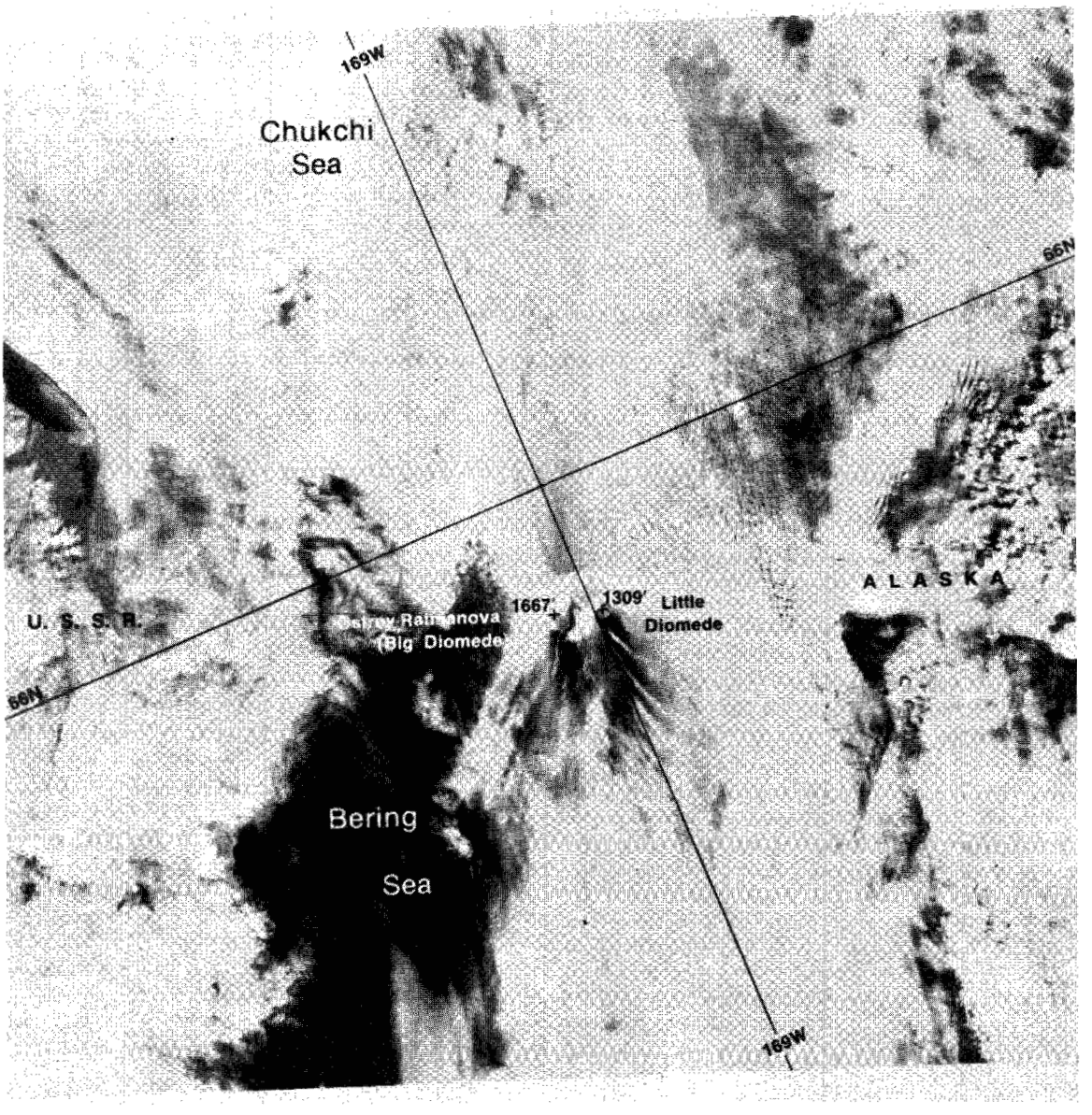

Figure 5. Shock waves off the Diomede Islands in the Bering Sea (Landsat-1, August 21, 1972, 1029-22212).

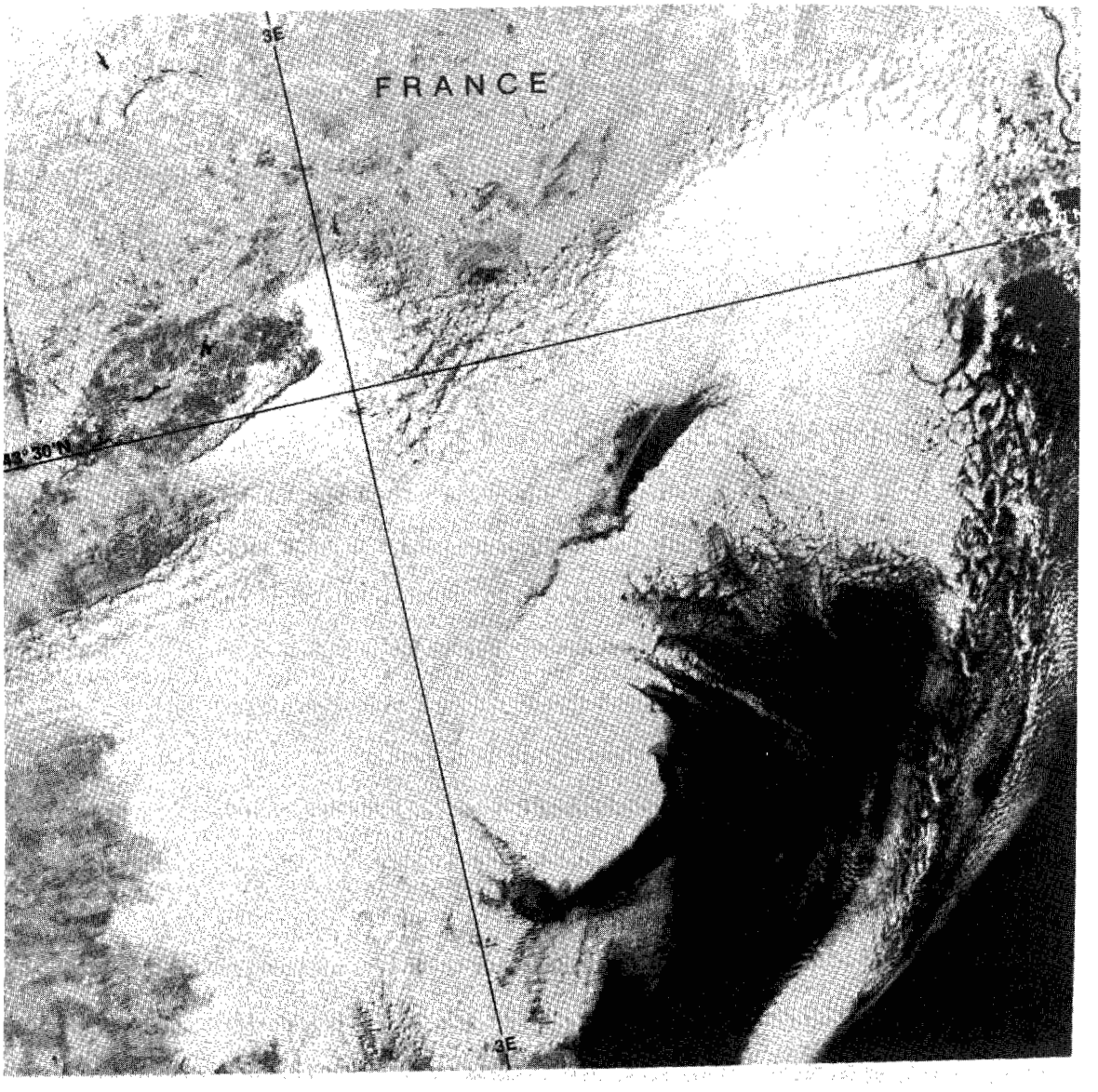

Figure 6. Cloud vortex in the Bay of Lions south of France (Landsat-1, May 14, 1973, 1295-10031).

LAYER CLOUDS PRODUCED BY RANDOM STIRRING MOTIONS

Fog and/or stratus may be produced by one of two processes: the cooling of the surrounding air to its dewpoint, or the addition of moisture into the air, which raises its dewpoint. Sufficient radiative cooling of the surface may occur on calm, clear nights, which in turn cools the air near the surface. Usually mixing takes place, which extends the cooling through a greater depth. Consequently, with sufficiently damp air or cooling, a fog of several hundred feet may result. The air may also be cooled in another way, that is, when air is moved horizontally (advected) over a cooler surface, giving up heat and producing advection fog. This type of cooling generally occurs over water or along coastlines where cooler surfaces over which moist air may be advected more commonly occur. The second fog-producing process, the addition of moisture, may occur along frontal zones, when rain from warm air aloft falls into a layer of cool air below. Evaporation from the raindrops may produce low stratus, and sometimes, fog (Reference 9).

Stratus clouds may also be formed due to the distribution of surface cooling upwards by moderate to strong winds. Due to radiational cooling from the upper surfaces of thin fog and stratus decks, irregular convection within the cloud layer produces wavelike features which Mason (Reference 3) calls billow clouds.

Figure 7 illustrates an example of billow clouds in the altocumulus cloud deck. The deck is aligned northwest of the Aleutian Range which runs along the southern side of the Alaskan Peninsula. A low was situated to the southwest, approximately 160°W, 56°N (off the image) producing southeast winds in the region of the frame. On the 0000 GMT July 17, 1973, 850-, 700-, and 500-mb charts, the winds at these levels in the area were from the east southeast at 2.6, 12.9, and 20.6 m/s (5, 25, and 40 knots), respectively, indicating little directional shear and significant vertical shear. Mason (Reference 3) states that uniformly distributed "dapples" (stratocumulus, altocumulus, or cirrocumulus) occur when the wind is almost the same throughout the cloud layer, but (as in this case) when the wind changes speed and/or direction with height, the globules become arranged in lines or rolls.

Figure 8 shows a Landsat-1 frame extending from southern Oregon into northern California past Crescent City and Redwood National Park. The North Pacific subtropical anticyclone and the cool coastal waters resulting from the anticyclonic circulation pattern produce ideal conditions for the fog and low stratus which frequently occur along the California coast. The northerly winds blowing around the east side of the high, which in this case were 5.1 to 7.7 m/s (10 to 15 knots), produce upwelling of cooler ocean water near the coast. This produces low-level stability, while subsidence maintains stability aloft (Reference 10). These areas of upwelling can be seen by the persistent cloud cover along the coast. Inland, the cooling effect is offset by the warmer land which heats up the surface air and dissipates the fog/stratus. The advection of warmer, moister air from farther offshore due to the prevailing winds provides a continual source for the formation of these coastal fogs.

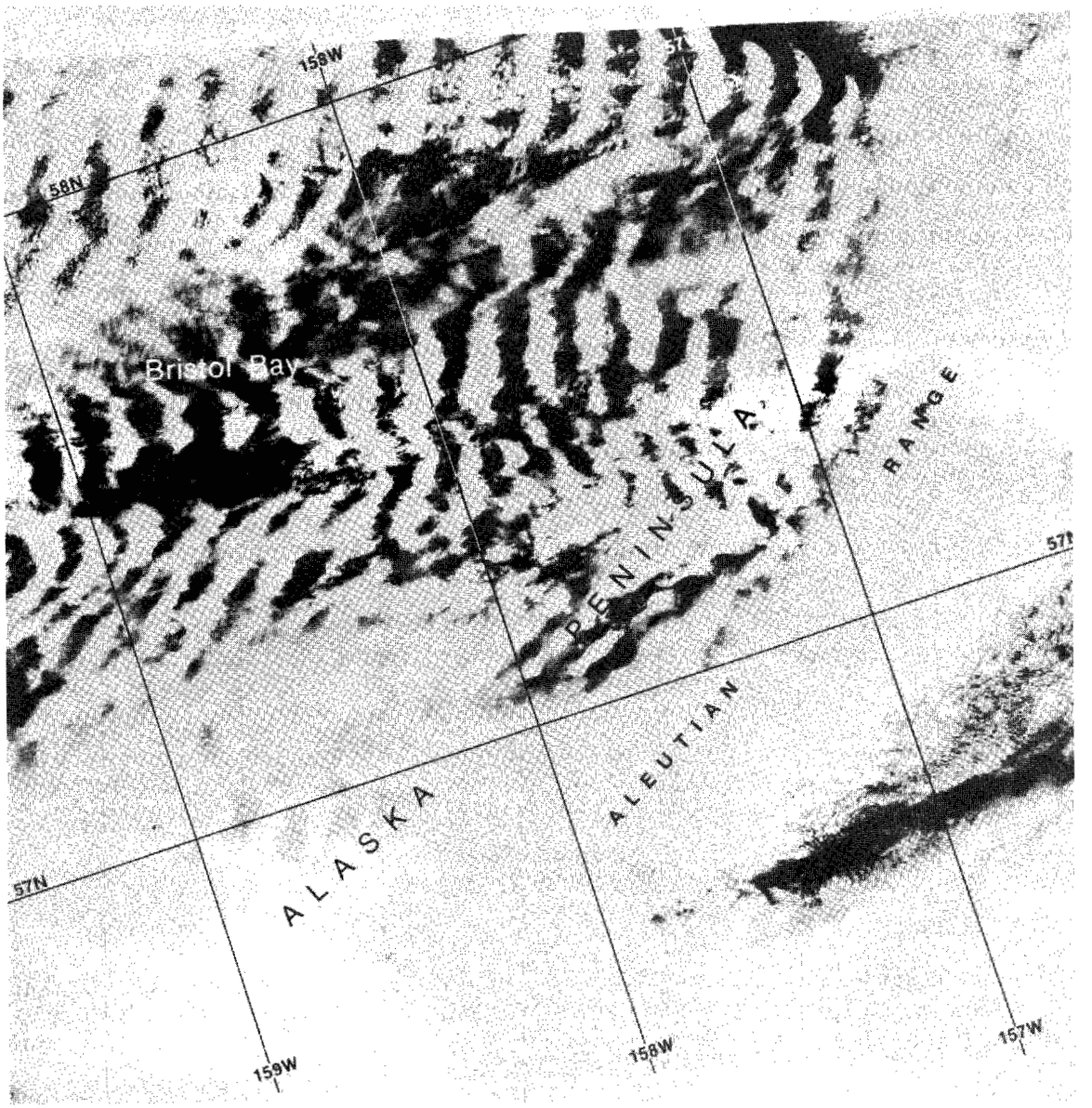

Figure 7. Billow clouds forming north of the Aleutian Range (Landsat-1, July 16, 1973, 1358-21093).

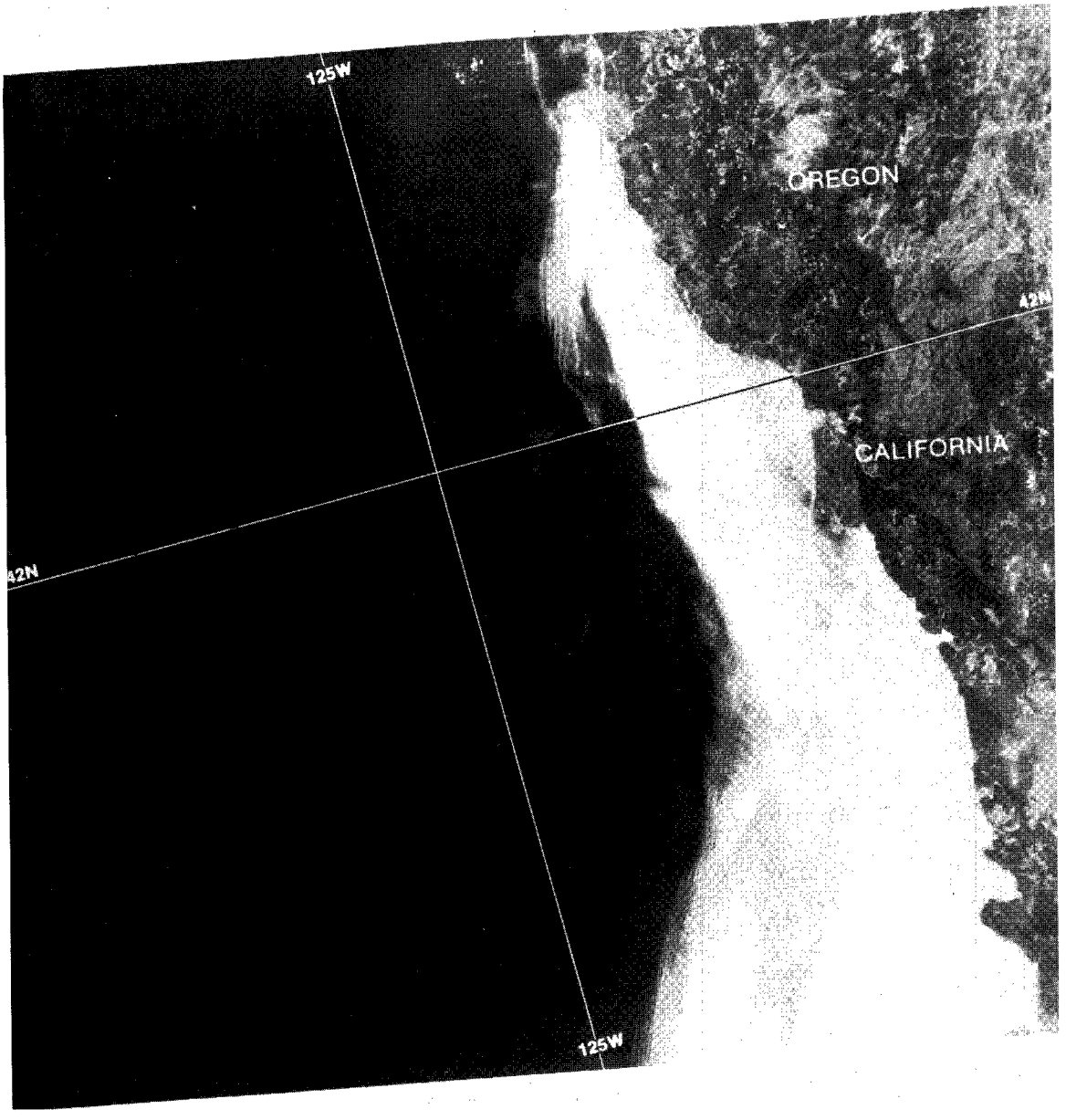

Figure 8. Stratus along the California and Oregon coasts (Landsat-1, May 13, 1973, 1294-18342).

CONVECTIVE CLOUDS

Convective clouds are the cumuliform clouds usually produced by rising plumes of air called thermals. On days when the air is rather stable, small well-scattered cumulus clouds may appear and persist throughout the warmer hours of the day. With more unstable conditions, these cumulus may grow to heights of 10 km or more, stopping only upon reaching the stable stratosphere. These two extremes are depicted here in Landsat imagery.

The sea breeze is a common phenomenon occurring along coastal waterways and large lakes during the warmer hours of the day (usually beginning around 10 a.m.). The land heats the air above, causing the air to expand and change the heights of the isobaric surfaces (Reference 11). Air then flows out over the cooler water from the upper surface of the heated air. As a result, pressure is increased over the water and decreased over the land, setting up a partial convectional circulation along the shore.

The result of the convectional circulation can be seen in figure 9 from Ft. Pierce, southward. The clouds of this incipient sea-breeze front range from 0.7 to 1.3 km from shore. Due to the time of day the Landsat imagery was obtained (~1030 local standard time (LST)), only the onset of the circulation overland can be seen.

Blair and Fite (Reference 11) indicate that a sea-breeze circulation is incomplete because the air from the top that flows out over the ocean spreads out broadly with a slow downward motion and is distributed over a large area. This downward outflow over the ocean can be seen east of Ft. Pierce, producing a buildup of small cumulus some 34 km from shore. As the land becomes warmer, the clear portion extending inland from the coast should increase to approximately the same distance as the clear area over water.

A smaller scale lake-breeze flow occurs northwest of Lake Okeechobee (at A). Its circulation is insufficient at this time, or the lake is too small to result in convective build-up over the water as a result of the return flow. The dampening effect of the cooler water on cloud growth is visible along the eastern shore of Lake Okeechobee.

Dynamically, only a shallow layer of the air is affected, for the sea breeze is usually 240- to 370-m deep (Reference 11). This shallowness is verified by the uninterrupted appearance of the cirrus band (B-B) extending from the eastern shore of Lake Okeechobee to the eastern extent of the image, and by the lower larger cumulus along the Atlantic coast southeast of Lake Okeechobee.

One of the more common mesoscale features seen on satellite images is cumuliform cloud streets or lines. Cloud streets, at first glance, appear to be a good indicator of low-level winds. Unfortunately, cloud-line orientations as seen in satellite images have been found to be not only parallel or normal to the wind flow, but also parallel to the wind shear vector (Reference 12).

Figure 10 shows an excellent example of the differential heating effects of land and water, and the formation of cloud streets over the warmer ocean surface as cold air streams off the continental land mass.

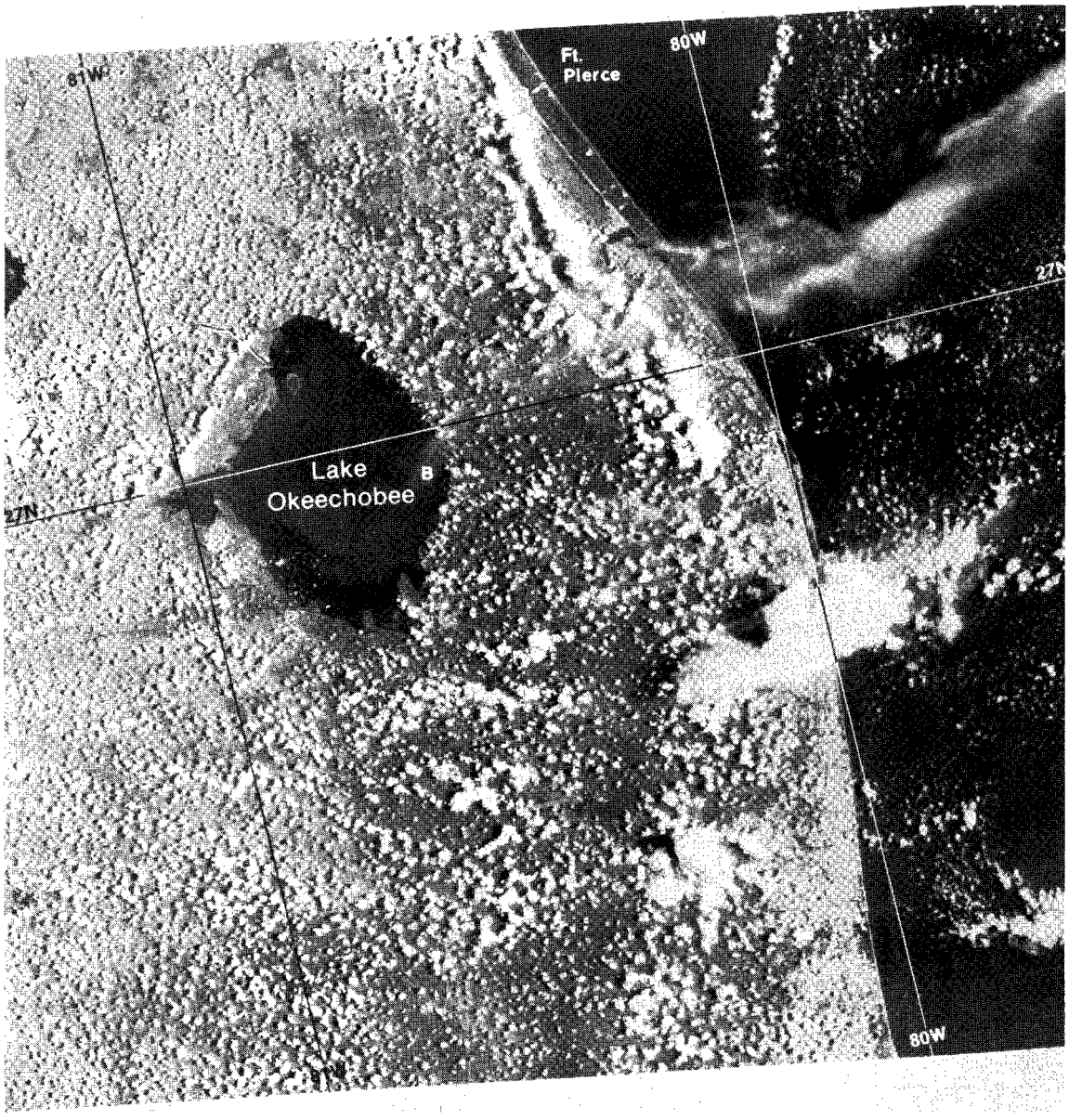

Figure 9. Sea-breeze front clouds along Florida coast
(Landsat-1, August 18, 1972, 1026-15223).

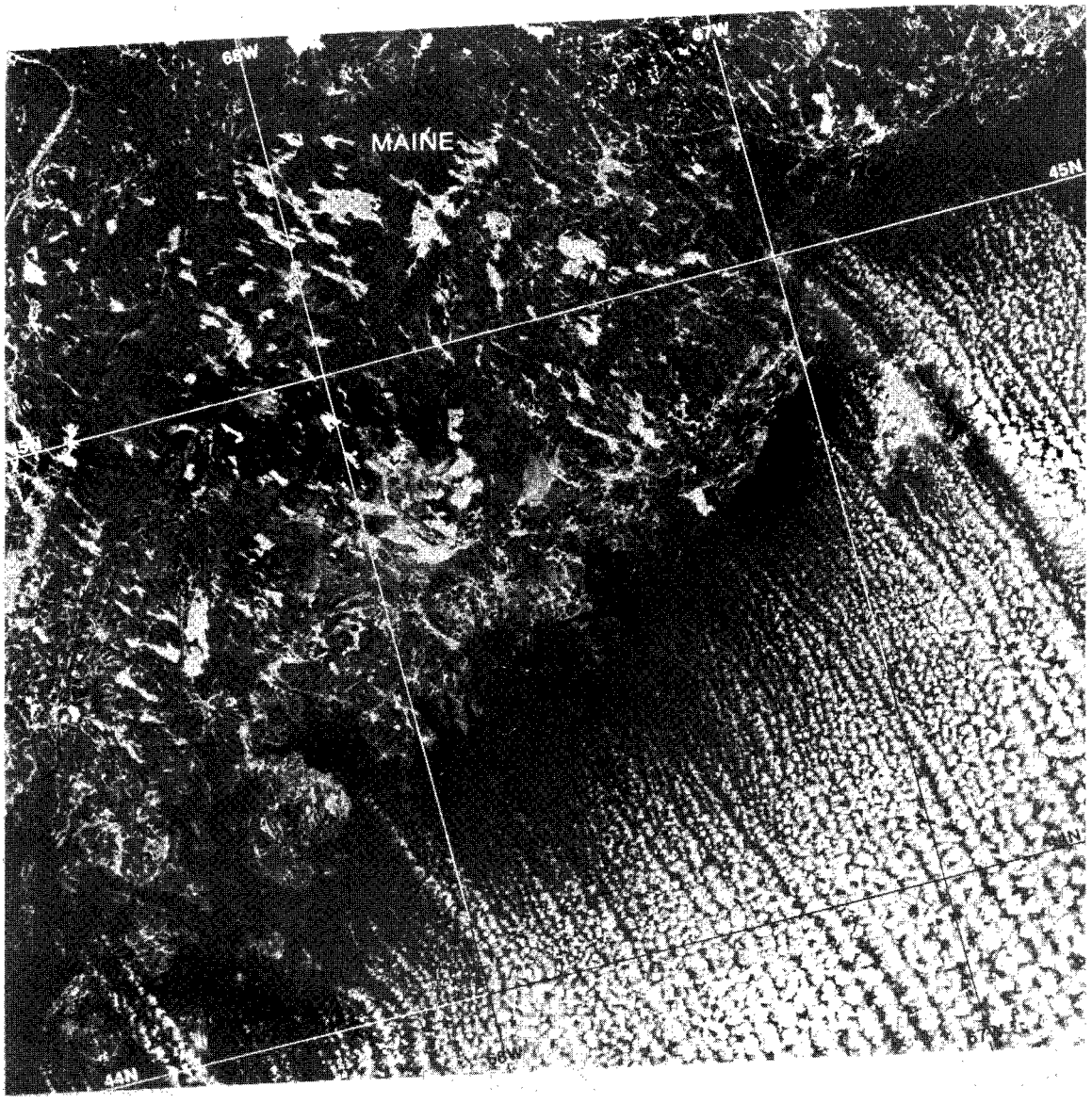

Figure 10. Cloud streets forming off Maine coast (Landsat-1, January 17, 1974, 1543-14453).

The 1500 GMT surface chart shows a large high (1040 mb) over James Bay. This had pushed a sharp cold front ahead of it which extended southwestward from a low at 49° W 41° N to 35° N near the U.S. east coast. The surface winds off the New England coast range up to 7.7 m/s (15 knots). A ship (38° N, 71° W) reported winds at 15.4 m/s (30 knots).

As the cold air -23° C (-10° F) and less with dewpoints -31° C (-23° F) and less, flows out over the warmer water, the dramatic effects of this abrupt change in temperature and moisture can be seen. This banding occurs southward along a good portion of the east coast of the United States (at least to 36° N 70° W where Landsat data ended).

The cloud bands (Reference 13) initially form as individual cumulus clouds which grow rapidly in size downwind of the coast. At their inception, these bands follow the surface wind direction. As the cumulus grow vertically, there may be a tendency for the cloud bands to be oriented parallel to the vertical wind shear (Reference 4).

A rather isolated cumulonimbus (Cb) cloud occurred about 100 km north northwest of Albuquerque, New Mexico, on July 28, 1973 (figure 11). A sharp boundary is prominent on the upwind side of the cloud, indicating active growth of the cloud. A small cirrus anvil extends approximately 35 km downwind from the apparent center of the main Cb. Other extensive cirrus cover most of the frame.

On the 1800 GMT July 28, 1973, weather map, Albuquerque, the closest station, was reporting surface winds of approximately 5 knots out of the southwest with low, middle, and high clouds. The low clouds consisted of cumulonimbus having a clearly fibrous (cirriform) top, often anvil-shaped, with or without cumulus (Cu), strato-cumulus (Sc), stratus (St), or Scud. The middle clouds consisted of gradually spreading and thickening altocumulus (Ac), with higher cirrostratus (Cs) covering the entire sky.

A rather undefined pressure pattern existed over most of the western United States at this time. The 12 GMT radiosonde and rawinsonde observations (RAOBS) taken at 50-mb intervals from the surface up to 200 mb are shown in figure 12. The direction of the cirrus blow-off, approximately 230°, agrees very well with the wind direction above 450 mb. In fact, there was both a directional and speed shear between 500 and 450 mb. This shearing may account for the cloud growth. Above this level, the winds remained from about the same direction, but increased to 29 m/s (~56 knots) at 200 mb. This cloud probably only extends to the 200-mb level and slightly beyond as the winds begin to veer at 175 mb and at 100 mb are from the west northwest at 6 m/s (11.6 knots).

CLOUDS FORMED BY OROGRAPHIC DISTURBANCES

When air is forced to ascend over an obstacle, turbulent flow may result, causing the wave form produced to extend several kilometers to the lee of the initiating source. Depending on the atmospheric moisture conditions, the crests of these wave forms are indicated by the position of the clouds. The following Landsat images illustrate simple orographic phenomena (cap clouds/hill fog) and the more complex or important lee waves.

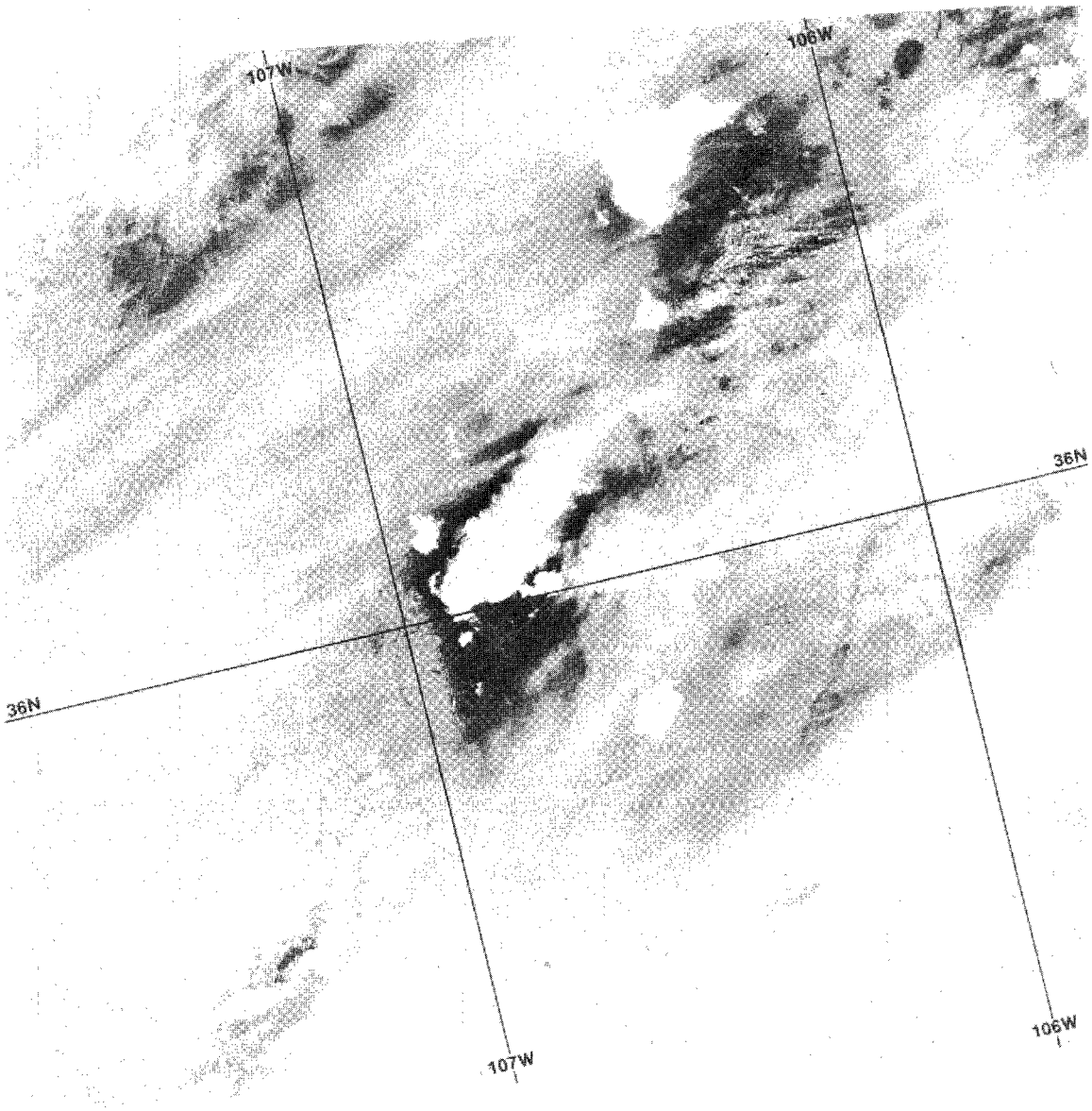

Figure 11. Isolated cumulonimbus north of Albuquerque, New Mexico (Landsat-1, July 28, 1973, 1370-17144).

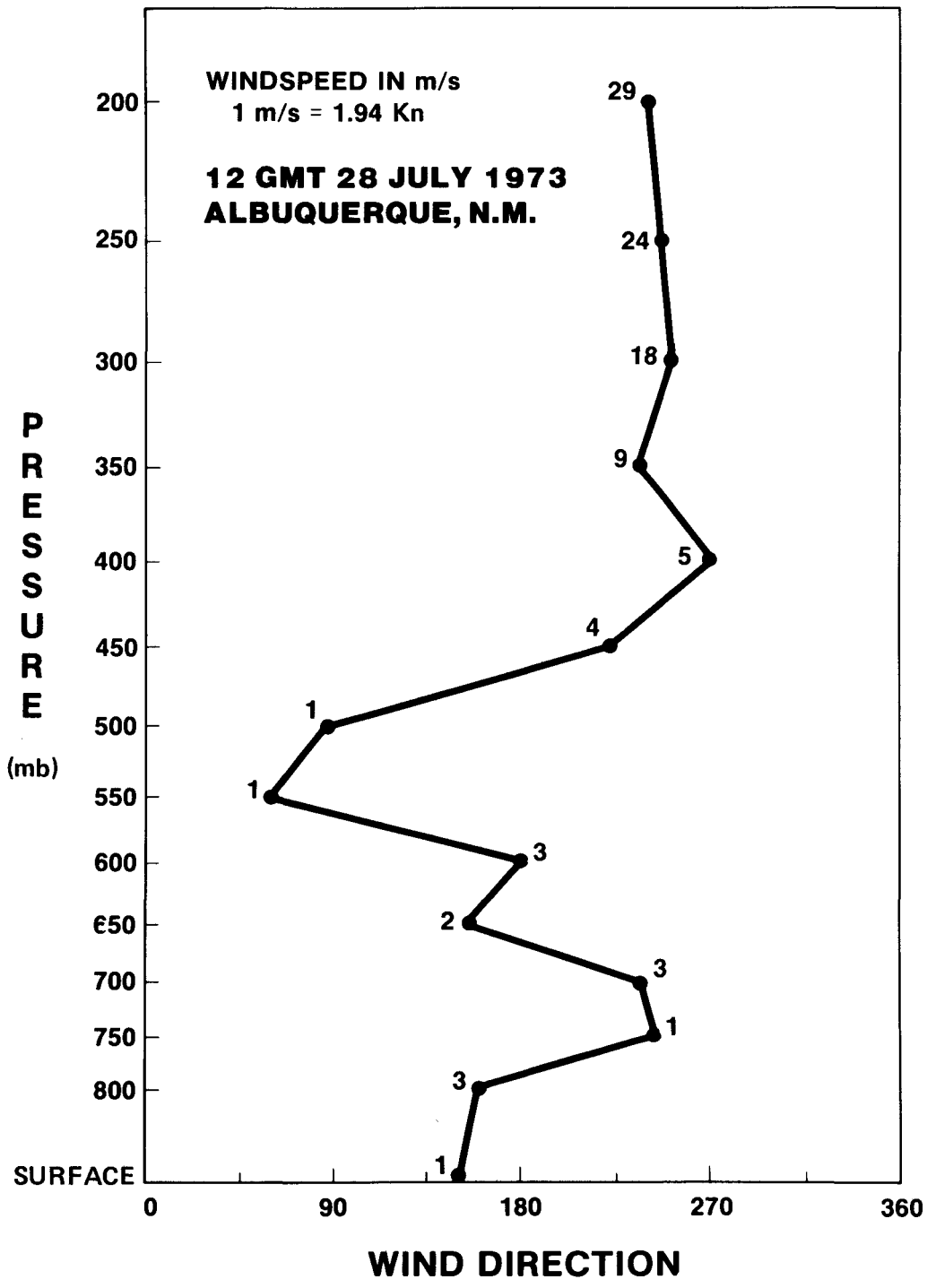

Figure 12. Wind profile over Albuquerque, New Mexico (12 GMT, July 28, 1973).

Cap clouds are the simplest example of forced ascent leading to saturation and cloud formation. Generally, hill fog forms over high ground which is influenced by maritime air masses. Less frequently, as in the case of an isolated conical mountain with laminar airflow, the cap cloud may form a symmetrical lenticular cloud or stack of shallow lenticulars resting on the mountain top. This form is an indication of stable stratification and nonturbulent flow (Reference 14). More frequently, cap clouds form as cloud sheets over extensive mountain ranges with their bases near or below the mountain tops. They may be several thousand feet thick with the upper surface frequently reflecting the shape of the ridge below. Although most of the cloud occurs over and windward of the mountain tops, it oftens descends the lee slope in the form of long streamers which are evaporated by adiabatic warming. These clouds are a feature of the turbulent friction layer over rugged terrain (Reference 14).

An excellent example of the latter description is seen in figure 13. The Sangre de Cristo Mountains in south central Colorado are blanketed by cap clouds that extend roughly the entire length (over 90 km) of the range. A sharp boundary occurs on the windward side with extensive streamers extending down the lee side (A).

The Sangre de Cristo Mountains extend over ~3660 m (12000 ft) with some peaks almost ~4260 m (14000 ft). On this particular day, a region of high pressure (1033 mb) was located over Idaho with a weaker high (1013 mb) over Kansas. Surface winds were from the northwest at 20 knots, increasing and backing to the west with height.

An excellent example of hill fog is seen in figure 14. Here the islands of San Nicolas and San Clemente are almost completely covered with a cap cloud. Distinct streamers can be seen extending downwind approximately 7 km. The surface winds were light but increased to over 51.5 m/s (100 knots) at 200 mb. The cirrus pattern (A-A) between the two islands is indicative of strong upper winds and possibly noticeable turbulence as indicated by the cloud trails and banding within the cirrus layer (Reference 7).

Wave cloud patterns (mountain waves/lee waves) are large-scale disturbances in the horizontal air flow which develop as standing wave patterns downstream of orographic barriers. They are termed standing waves because the wave form remains approximately stationary, that is, the wind blows through the pattern (Reference 14). Several conditions govern their formation, magnitude, and extent. Meteorologically, one needs atmospheric stability and wind speeds of at least 7 to 15 m/s (13.6 to 29.1 knots). Stable stratification occurs when the actual lapse rate is less than the adiabatic lapse rate. As a result, an air parcel subjected to a vertical displacement attempts to regain its equilibrium with gravity-inertia forces tending to cause oscillations of the parcel about its equilibrium position (Reference 14).

Topographically, while lee or mountain waves generally occur downwind of major mountain barriers (figure 15) which are oriented roughly normal to the low-level flow, hilly terrain with ridges as low as ~100 m (300 ft) may initiate disturbances (Reference 15). Alaka (Reference 14) states that the vertical displacement of the airstream may be caused otherwise than by a mountain, for example, by a valley. Indeed, the presence of a material obstacle is not essential (figure 16) and equivalent effects can be produced by a wedge of cold air or by differential heating (figure 17).

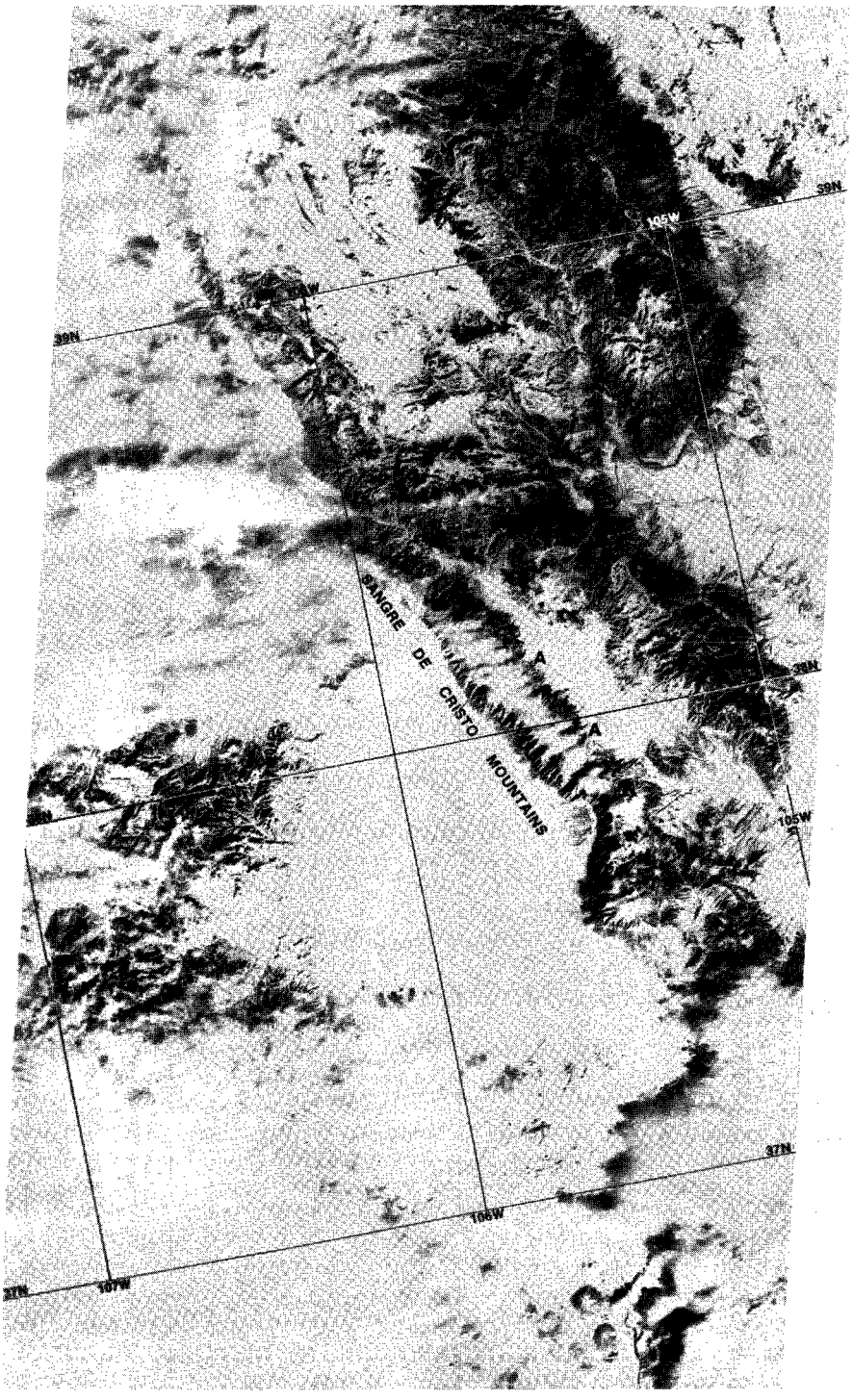

Figure 13. Cap cloud on the Sangre de Cristo Mountains (Landsat-1, January 6, 1974, 1532-17110, 17113).

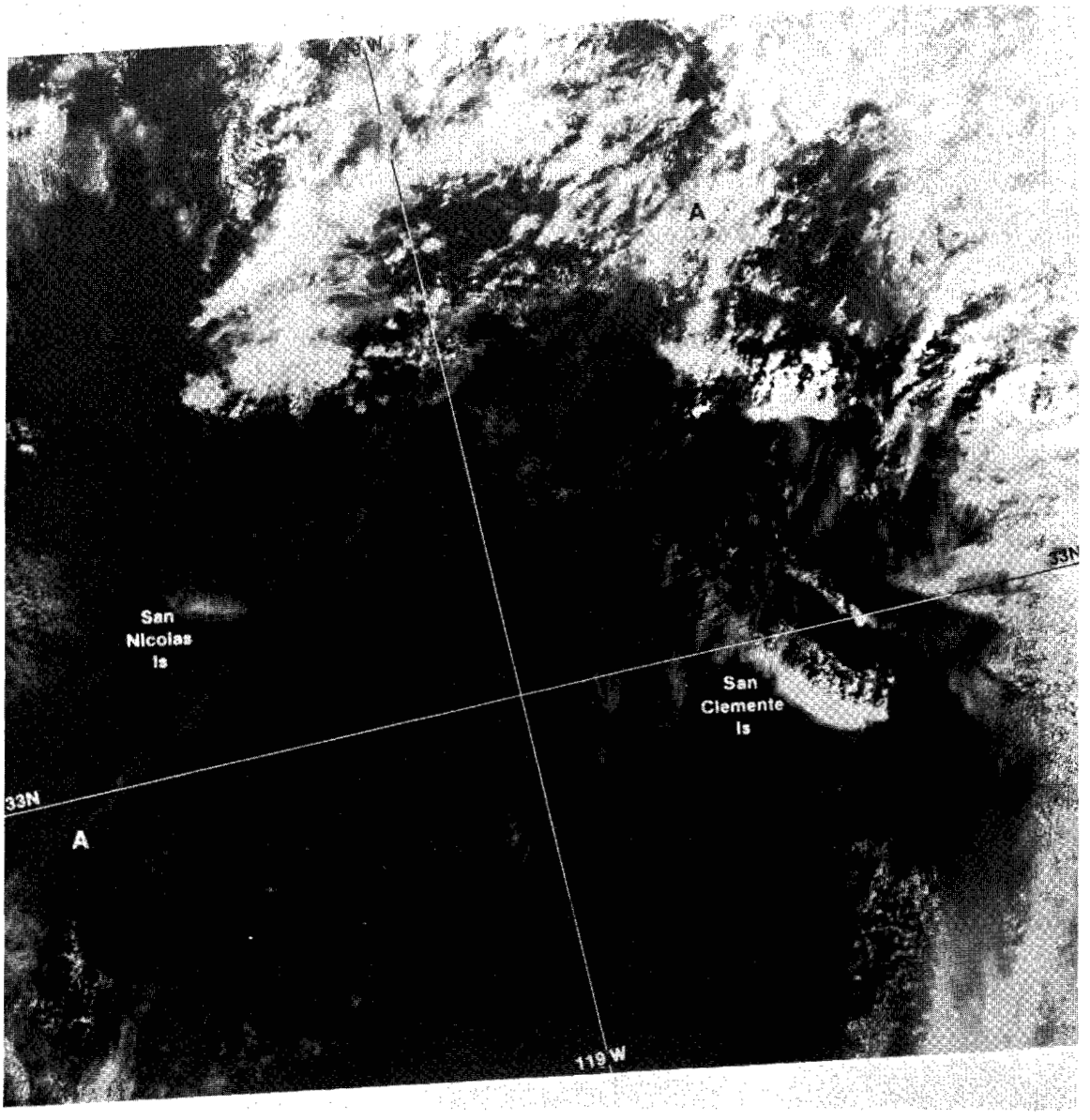

Figure 14. Hill fog over San Nicolas and San Clemente Islands (Landsat-1, February 6, 1973, 1198-18021).

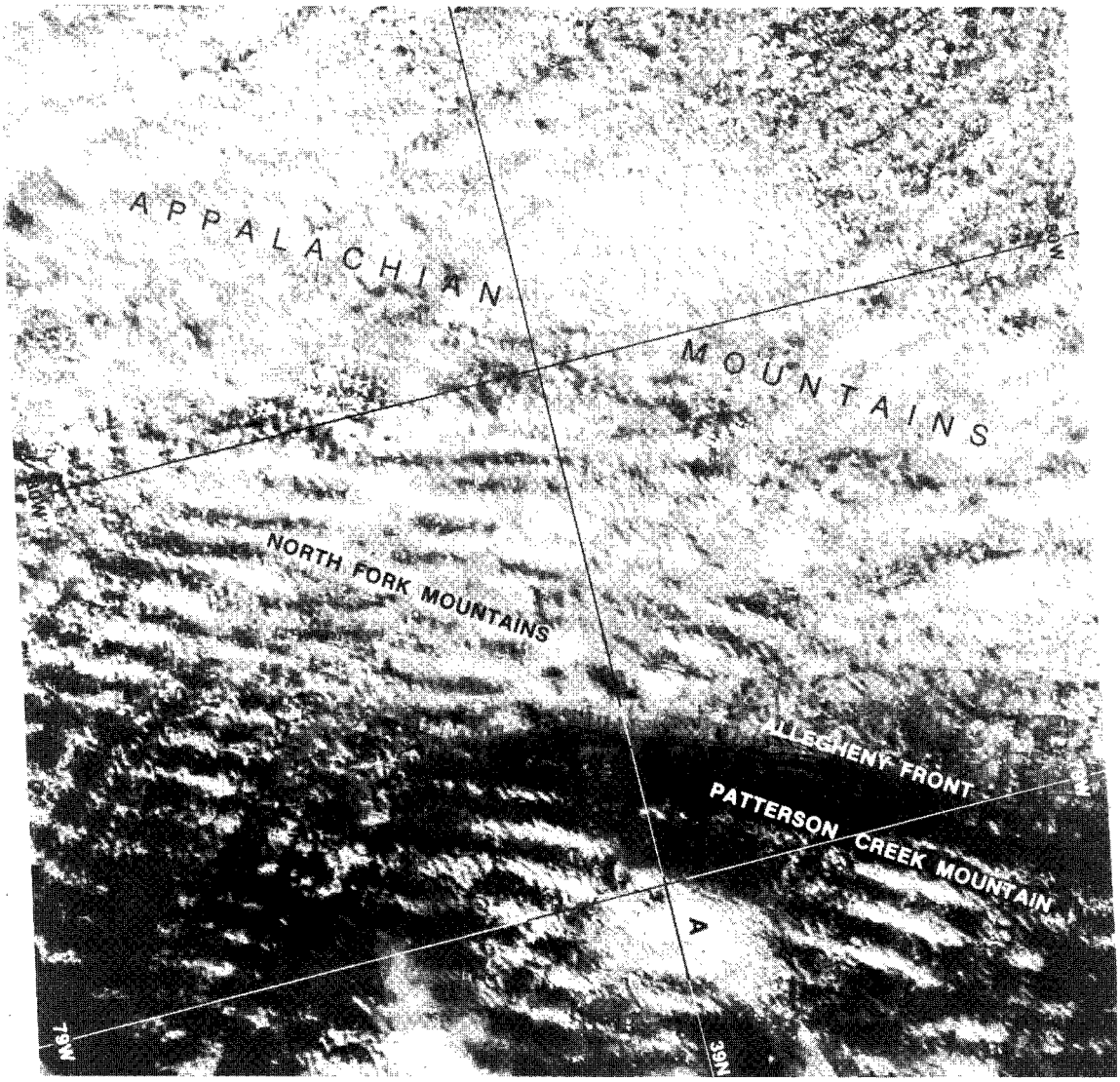

Figure 15. Wave clouds induced by Appalachian Mountains (Landsat-1, January 29, 1973, 1190-15311).

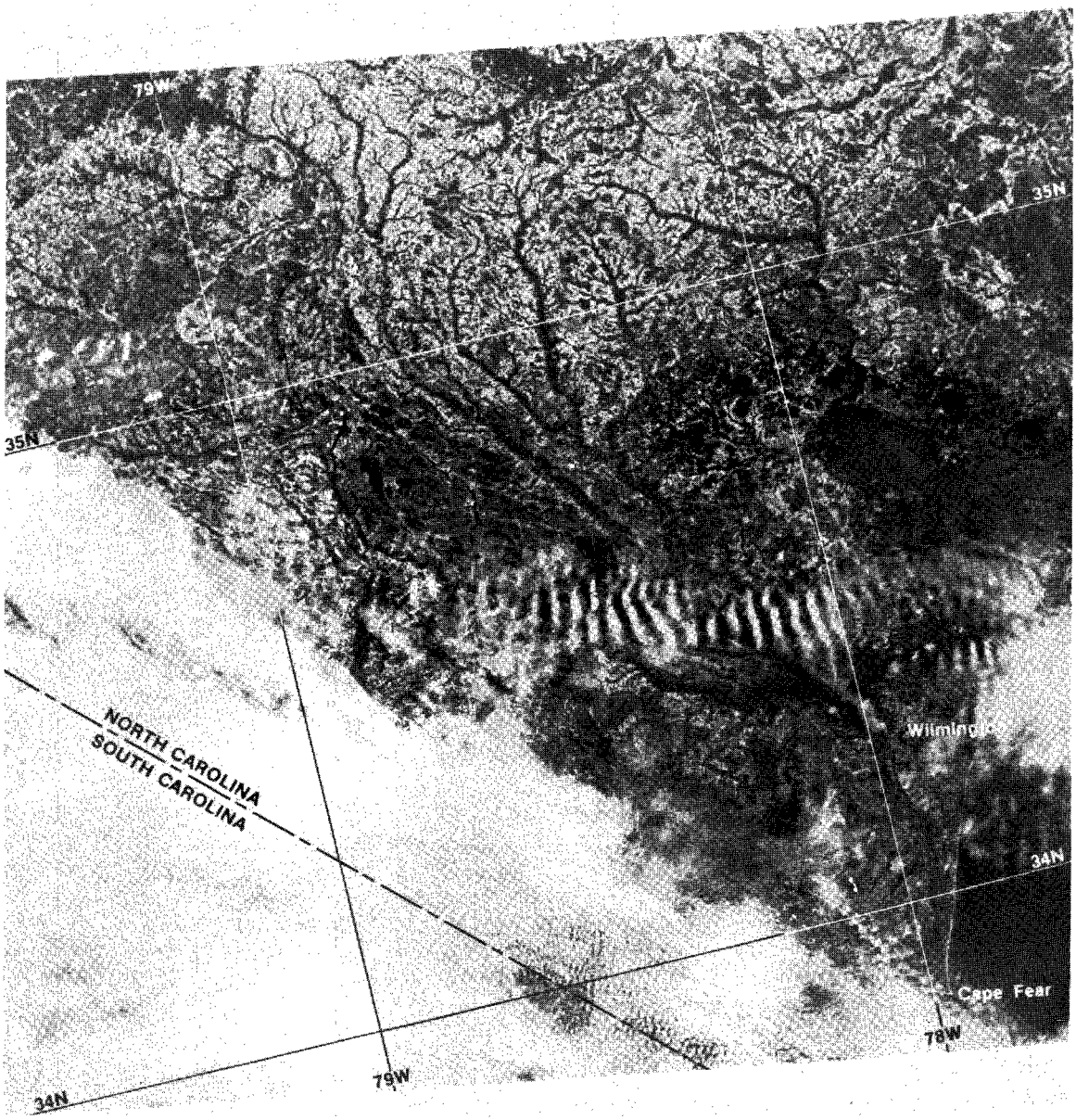

Figure 16. Wave clouds in southern North Carolina (Landsat-1, April 29, 1976, 5376-14384).

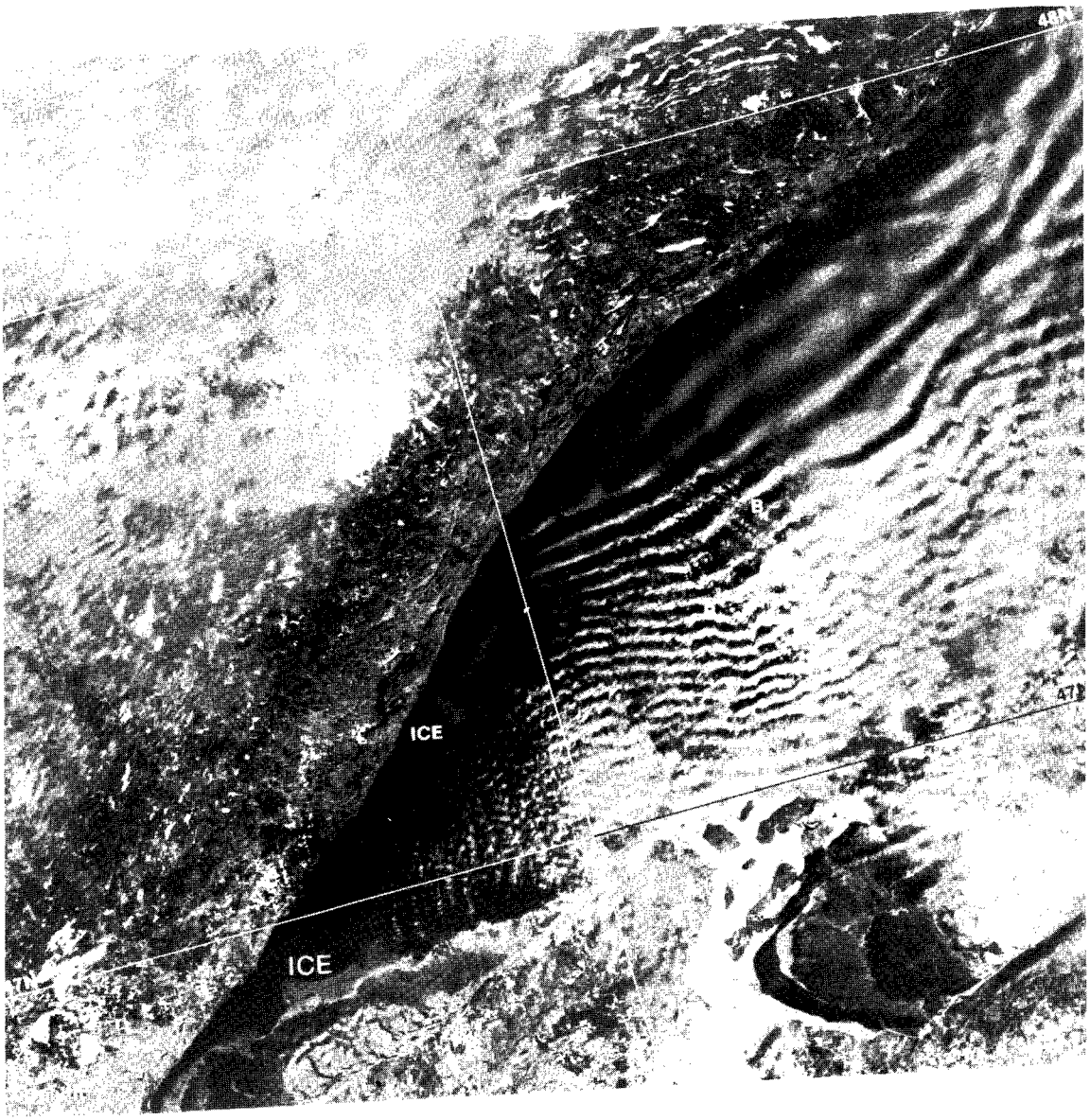

Figure 17. Wave clouds over Lake Superior
(Landsat-1, February 8, 1973, 1200-16262).

The wavelength is governed by the wind component normal to the obstacle, the upstream vertical temperature gradient, and the configuration of the obstacle itself. Stable flow nearly always exists above (hundreds of meters) the obstacle with an increase in flow with height. Stronger winds contribute to large wave amplitudes and subsequently greater vertical displacement (References 14 and 15).

As indicated above, three Landsat frames have been chosen to illustrate lee wave phenomena as seen in the mesoscale. The scene depicted in figure 15 (January 29, 1973) covers portions of West Virginia, Virginia, and western Maryland. The waves are forming to the lee of the Allegheny Front and North Fork Mountain of the Allegheny Mountains. The mountain crest ranges from 760 m (2500 ft) in the Allegheny Front to 1080 m (3550 ft) in the North Fork Mountain region. To the lee, elevations are 300 m (1000 ft) less. A small ridge, 455 m (1500 ft), may be producing the cloud mass at "A".

An occluded low was positioned off the eastern end of Long Island (41° N, 72° W), producing 5.1- to 7.7-m/s (10- to 15-knot) surface winds from the north. Aloft, the winds backed to the west at 850 mb and then veered to the northwest at 700 mb and remained from that direction increasing in velocity with height.

Farther south, figure 16 (April 29, 1976) covers a portion of southwestern North Carolina and the adjacent northeastern portion of South Carolina. Cape Fear is in the lower right corner. The whole area is coastal plain with very little relief. Near the point of wave inception, elevations are up to ~45 m (150 ft), dropping down to ~15 m (50 ft) to the east.

On April 29, 1976, the 1500 GMT synoptic weather chart showed a high over central Illinois. Surface winds along the Carolinas' coast were out of the northeast at 2.6 m/s (5 knots). At higher altitudes, the winds backed to west northwest increasing from 20.6 m/s (40 knots) at 500 mb to 30.9 m/s (60 knots) at 200 mb.

This example is unusual in that no large obstacle is present to initiate the disturbance, yet the wave phenomena persist over 70 km downstream. Just south of the above area, four distinct waves can be seen with many smaller waves overriding these larger waves.

Wave clouds, possibly induced by differential heating, can be seen in figure 17 (February 8, 1973). Weather maps indicated a large pool of cold air positioned over the western Great Lakes region. The surface temperatures near this portion of Lake Superior were below -12° C (-10° F), with the wind direction varying from west to northwest at approximately 5.1 m/s (10 knots). The winds increased with height and veered slightly from the northwest at 850 mb to north northwest at 500 mb. The wind speed increased somewhat from 10.3 m/s (20 knots) to over 18.0 m/s (35 knots).

Since the lake shows some ice floating on it, the surface temperature was inferred to be close to 0° C (32° F). Therefore, there was at least an 11° C (30° F) temperature difference between the water and the air streaming over it. At 'B', one can see several cloud streets; a thermally-induced cloud feature.

Alaka (Reference 14) states that ". . . it is possible to obtain a fair estimate of the lee wavelength, . . . in a simple fashion . . . . The relevant parameter expressing the dynamical state of the air stream at any level is given by

$$F(z) = \frac{\bar{\sigma} g}{\bar{u}^2}$$

where $\bar{\sigma}$ is the static stability and $\bar{u}$ is the horizontal wind speed. The theory indicates that the wavelength of any lee waves will be somewhere between the maximum and minimum values of $2\pi\sqrt{F(z)}$ or $2\pi\,\bar{u}/\sqrt{g\bar{\sigma}}$ through the troposphere." Since the mean stability does not vary through the troposphere, only from one air mass to another, we can assume a mean stability corresponding to about half the adiabatic lapse rate, and obtain for the lee wavelength:

$$\lambda = 1/2\,\bar{u}$$

where λ is in km and $\bar{u}$ is in m/s. Using this simple algorithm on the three scenes, we come up with the following comparison that is shown in table 1.

Table 1

Comparison Between Theoretical and Landsat-estimated Lee Wave Wavelengths

	$\bar{u}$ *m/sec	λkm	Landsat λkm
29 January 1973	12	6.0	6.7
29 April 1976	16	8.0	3.5
8 February 1973	18	9.0	3.4

*500-mb wind used.

In two of the three cases the theoretical λ is more than twice the λ measured from Landsat. The λ in closest agreement occurred for the January 29, 1973 case which more closely fits the situation under which the theory was developed. The April 29, 1976 case occurred under little topographical changes, and the February 8, 1973 case was thermally induced.

Rotor or roll clouds have the appearance of a line of Cu or Sc parallel to and downwind of mountain crests. The base is usually near the level of the crest while the top may extend several thousand feet higher. The term "rotor" refers to the actual rotational appearance the clouds usually have. Alaka (Reference 14) states that this is due to the large positive vertical wind shear through the cloud.

An excellent example of a roll cloud is seen in figure 18. The cloud is aligned with the continental divide in the Wind River Range in northwestern Wyoming. Elevations in the range reach ~4203 m (13785 ft) at Gannet Peak. While the outward appearance of the cloud in figure 18 fits the description, the large positive vertical wind shear through the cloud is not evident from the 12 GMT and 00 GMT constant pressure charts for August 12 and 13, 1976. The winds at or above 500 mb remained fairly uniform between 15 to 30 knots from the west to west southwest.

CONCLUSION

The Landsat system, although neither designed nor intended for use in daily, synoptic meteorological applications, does offer sufficiently detailed images using high spatial resolution to provide some intriguing insight into such mesoscale features as jet cirrus, vortices (Kármán), shock waves, land/sea-breeze effects, cloud banding, and wave clouds. Further investigations into the dynamics of these phenomena could profitably include Landsat imagery.

ACKNOWLEDGMENTS

I would like to thank Dr. Robert Adler and Mr. Edward Rodgers for their many helpful suggestions during preparation of text for the images selected. I would also like to express my appreciation to Mr. James Foster and many other people who furnished me with interesting Landsat cloud features. Special thanks go to Dr. Philippe Schereschewsky for his most helpful discussion on mesoscale cloud forms.

Goddard Space Flight Center
National Aeronautics and Space Administration
Greenbelt, Maryland April 1977

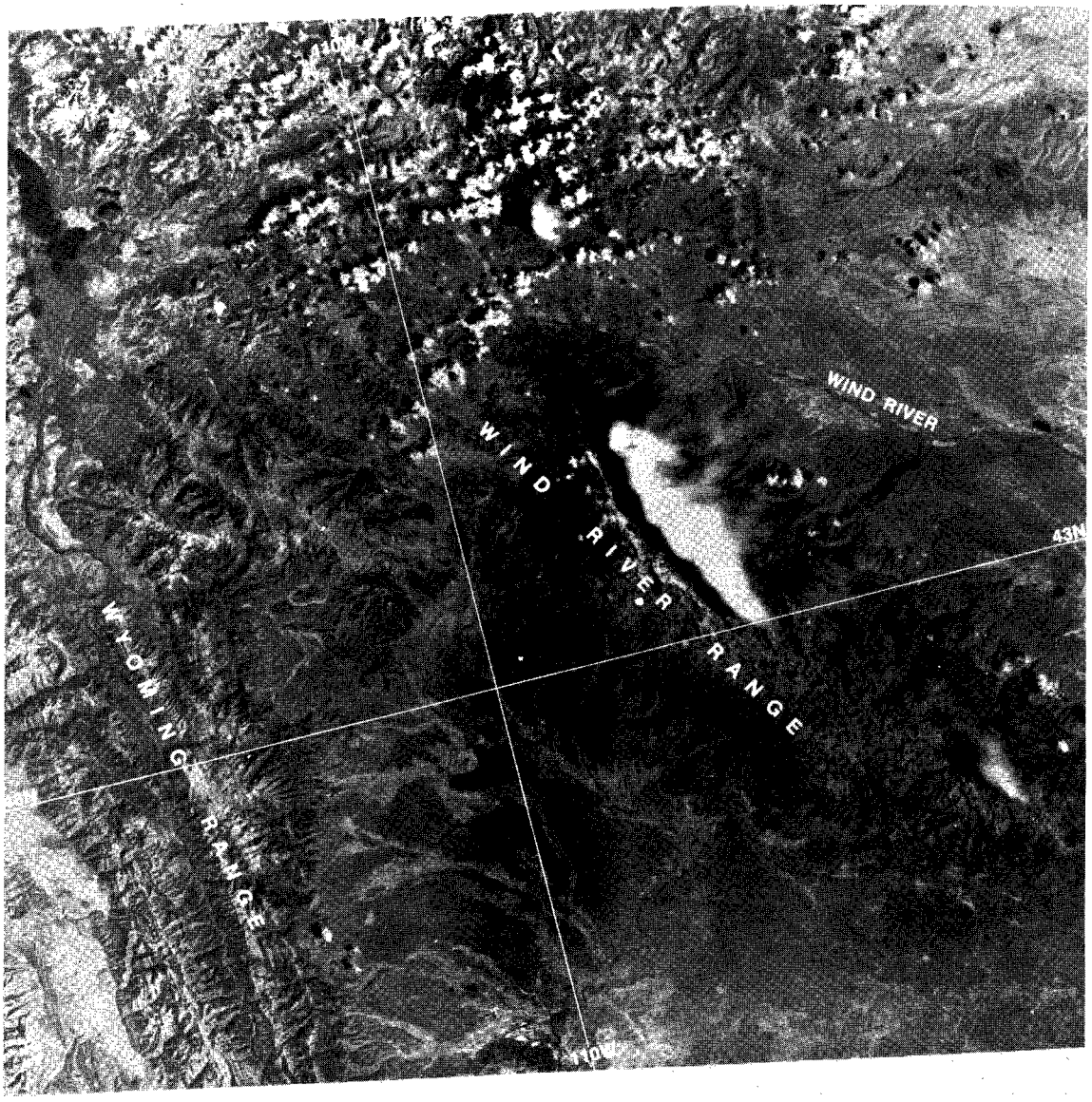

Figure 18. Rotor cloud over the Wind River Range, Wyoming (Landsat-2, August 12, 1976, 2568-17162).

REFERENCES

1. Boeckel, John H., "ERTS-1 System Performance Overview," *Third ERTS-1 Symposium,* NASA/Goddard Space Flight Center, Washington, D.C., December 10-14, 1973.

2. *International Cloud Atlas*, World Meteorological Organization, Geneva, Switzerland, 1956.

3. Mason, B. J., *Clouds, Rain and Rain Making*, Cambridge University Press, Great Britain, 1962.

4. Anderson, R. K., E. W. Ferguson, and V. J. Oliver, *The Use of Satellite Pictures in Weather Analysis and Forecasting,* World Meteorological Organization Technical Note No. 75, WMO - No. 190, TP. 96, Geneva, Switzerland, 1966.

5. Chopra, K. P., and L. F. Hubert, "Mesoscale Eddies in Wake of Island," *J. of Atmos. Sci.*, 1965, 22, (11), pp. 652-657.

6. Reiter, E. R., *Jet Stream Meteorology*, The University of Chicago Press, Chicago and London, 1961.

7. Anderson, R. K., et al., *Application of Meteorological Satellite Data in Analysis and Forecasting,* Reprint of ESSA Technical Report NESC 51, NOAA/NESS, Washington, D. C., 1974.

8. Boucher, Roland J., and Ralph J. Newcomb, "Synoptic Interpretation of Some TIROS Vortex Patterns: A Preliminary Cyclone Model," *J. Appl. Meteorol.*, 1, 1962, pp. 127-136.

9. Pettersen, S., *Introduction to Meteorology*, McGraw-Hill, New York, 1969.

10. Trewartha, Glen T., *The Earth Problem Climates*, The Univ. of Wisconsin Press, Madison, Wis., 1966.

11. Blair, Thomas A., and Robert C. Fite, *Weather Elements*, Prentice-Hall, Inc., Englewood Cliffs, N. J., 1965.

12. Widger, W. K., Jr., P. E. Sherr, and C. W. C. Rogers, "Practical Interpretation of Meteorological Satellite Data," *Air Weather Service Technical Report 185,* Air Force Cambridge Research Laboratories Contract No. AF 19 (628)-2471, Aracon Geophysics Company, Concord, Mass., 1965.

13. Feteris, Pieter J., A. S. Lisa, C. J. Bowley, M. G. Fowler, and J. C. Barnes, "Investigation of Mesoscale Cloud Features Viewed by Landsat," Environmental Research and Technology, Inc., Concord, Mass., Document P-0619, Type 3 Report NAS5-20804.

14. Alaka, M. A., *The Airflow Over Mountains,* WMO Technical Note 34, Geneva, Switzerland, 1960.

15. Cole, F. W., *Introduction to Meteorology,* John Wiley & Sons, Inc., New York, 1970.